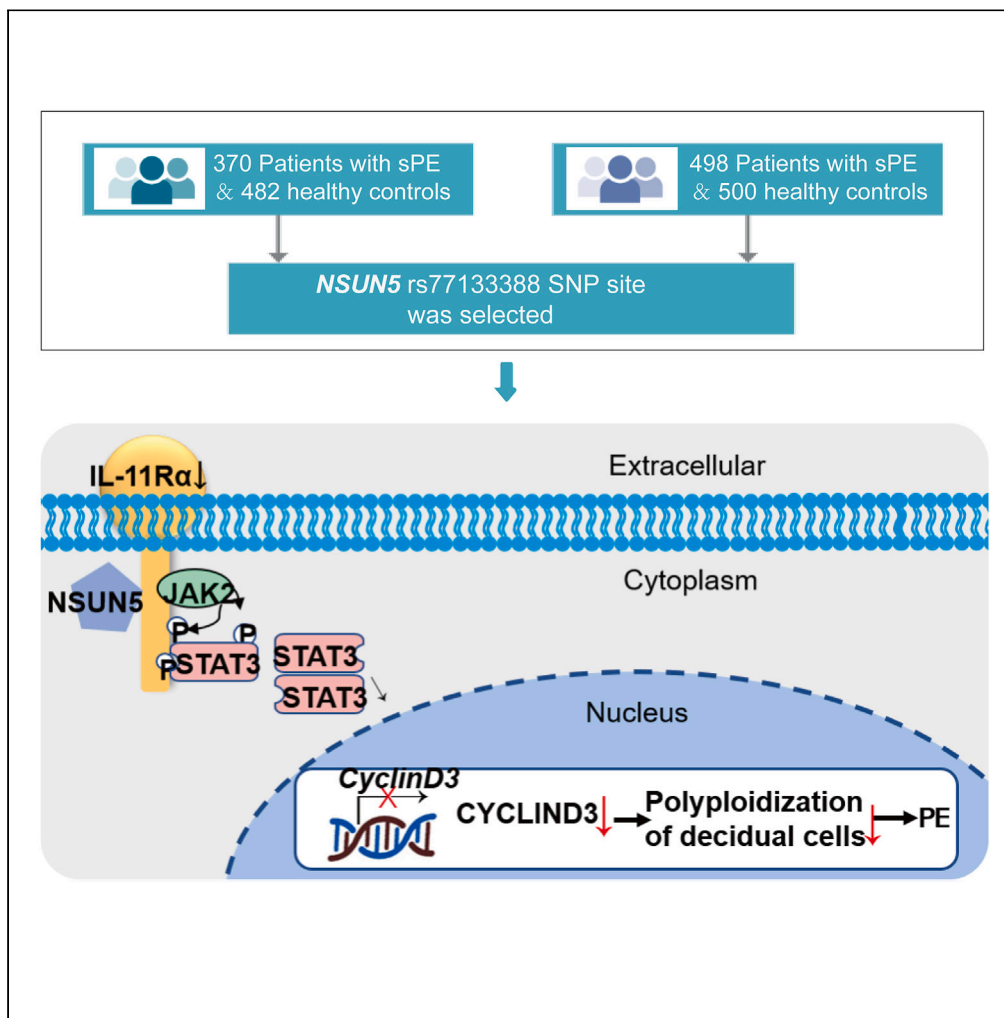


Article

The mutation of NSUN5 R295C promotes preeclampsia by impairing decidualization through downregulating IL-11R α



Hongya Zhang,
Huihui Li, Jiatong
Yao, Miaomiao
Zhao, Cong Zhang

zhangxinyunlife@163.com

Highlights

The SNP rs77133388 of NSUN5 is significantly associated with the risk of preeclampsia

The process of decidualization is impaired in NSUN5 R295C mice

The NSUN5 mutation promotes preeclampsia via IL-11R α /JAK2/STAT3/ Cyclin D3 pathway

Zhang et al., iScience 27,
108899
February 16, 2024 © 2024 The
Author(s).
[https://doi.org/10.1016/
j.isci.2024.108899](https://doi.org/10.1016/j.isci.2024.108899)



Article

The mutation of NSUN5 R295C promotes preeclampsia by impairing decidualization through downregulating IL-11R α Hongya Zhang,¹ Huihui Li,² Jiatong Yao,¹ Miaomiao Zhao,¹ and Cong Zhang^{1,3,4,5,6,*}

SUMMARY

Preeclampsia (PE) is a pregnancy-specific hypertensive disorder that severely impairs maternal and fetal health. However, its pathogenesis remains elusive. NOP2/Sun5 (NSUN5) is an RNA methyltransferase. This study discovered a significant correlation between rs77133388 of NSUN5 and PE in a cohort of 868 severe PE patients and 982 healthy controls. To further explore this association, the researchers generated single-base mutant mice (NSUN5 R295C) at rs77133388. The pregnant NSUN5 R295C mice exhibited PE symptoms. Additionally, compared to the controls, the decidual area of the placenta was significantly reduced in NSUN5 R295C mice, and their decidualization was impaired with a significantly decrease in polyploid cell numbers after artificially induced decidualization. The study also found a decrease in phosphorylated JAK2, STAT3, and IL-11R α , Cyclin D3 expression in NSUN5 R295C mice. Overall, these findings suggest that NSUN5 mutation potentially alters decidualization through the IL-11R α /JAK2/STAT3/Cyclin D3 pathway, ultimately impairing placental development and contributing to PE occurrence.

INTRODUCTION

Preeclampsia (PE) is a disease characterized by a new onset of maternal hypertension ($\geq 140/90$ mmHg) and/or proteinuria (≥ 0.3 g/L) after 20 weeks of gestation. This condition is a significant cause of maternal and fetal mortality and morbidity.¹ The global incidence rate of PE is 5%–8% of pregnancies.² Annually, it is estimated that approximately 46,000 maternal deaths and 500,000 fetal and newborn deaths are caused by this condition.³ Severe PE (sPE) can lead to eclampsia, stroke, clonus, severe headaches, pulmonary edema, hematological complications, acute renal injury, and uteroplacental dysfunction.^{3,4} Furthermore, it increases the risk of long-term chronic diseases for mothers and children.⁵ Despite extensive research, the biological basis of this disorder remains complex and multifactorial and not fully understood. Currently, the only definitive treatment available for this condition is the delivery of the placenta.⁶

In 2014, Redman proposed a widely accepted “six-stage model” to explain the pathogenesis of PE.⁷ According to this model and most studies, placental damage is the cause of the emergence of PE clinical symptoms. Other studies have suggested that alterations in the renin-angiotensin-aldosterone axis, immune maladaptation, oxidative stress, inadequate trophoblast invasion, and genetic factors contribute to PE occurrence.^{8–10} However, it should be noted that decidualization is the basis for placentation and growth.¹¹ When the mouse embryo implants, the rapid growth of the endometrial stromal cells is the earliest and most striking event in the uterine milieu, leading to the formation of special cells termed decidual cells. This process, known as decidualization is characterized morphologically by the transformation of elongated fibroblast-like cells into an enlarged polygonal or round shaped population involving complex cytoskeletal rearrangements.¹² The formation of decidua is critical for the initiation and maintenance of pregnancy.¹³ An increasing number of studies have shown that abnormal decidualization is an important factor in the occurrence of PE.^{14–17}

NSUN5 is a conserved RNA methyltransferase that belongs to the Nop2/sun domain family.¹⁸ Previous studies have reported the role of NSUN5 in human cancer, particularly in colorectal cancer, where it acts as a promotor of tumor development by regulating cell cycle processes.¹⁹ Additionally, the loss of NSUN5 leads to impairments in global protein synthesis and normal growth.¹⁸ Moreover, NSUN5 is critical for the normal morphology of the tetralogy of Fallot.²⁰ Its deletion is associated with the agenesis of corpus callosum observed in Williams-Beuren syndrome.²¹ Recent research suggests that NSUN5 plays an essential role in suppresses ferroptosis in bone marrow-derived

¹Shandong Provincial Key Laboratory of Animal Resistance Biology, College of Life Sciences, Shandong Normal University, Jinan, Shandong 250014, China

²Center for Reproductive Medicine, Department of Obstetrics and Gynecology, Qilu Hospital of Shandong University, Jinan, Shandong 250012, China

³Center for Reproductive Medicine, Ren Ji Hospital, School of Medicine, Shanghai Jiao Tong University, Shanghai 200135, China

⁴Shanghai Key Laboratory for Assisted Reproduction and Reproductive Genetics, Shanghai 200135, China

⁵Shandong Provincial Key Laboratory of Reproductive Medicine, Jinan, Shandong 250001, China

⁶Lead contact

*Correspondence: zhangxinyunlife@163.com

<https://doi.org/10.1016/j.isci.2024.108899>



Table 1. The baseline clinical characteristics of the study subjects in the severe preeclampsia (sPE) and healthy controls (HCs)

Variables	sPE (n = 868)	HCs (n = 982)	p value
Maternal age (years)	30.3 ± 5.6	27.2 ± 4.5	>0.05*
SBP (mmHg)	164.8 ± 13.7	118.7 ± 10.1	<0.01*
DBP (mmHg)	108.1 ± 14.0	75.2 ± 7.4	<0.01*
Gestational age at delivery (weeks)	36 ± 2.9	39. ± 1.3	<0.01*
Birth weight (g)	2634.9 ± 759.6	3408.7 ± 391.3	<0.01*
Proteinuria (+)	++~+++	NA	NA

Note: SBP, systolic blood pressure; DBP, diastolic blood pressure; NA, not applicable. *Student's t-test.

mesenchymal stem cells through interaction with TRAP1.²² However, little is known about the function of NSUN5 in other diseases and biological processes, particularly in the context of PE and decidualization.

Each person possesses multiple differences in the diploid genome. Most of which are a result of single base substitution polymorphisms, known as single nucleotide polymorphisms (SNPs).²³ These SNPs are single nucleotide variations in genome that can interrupt transcription and posttranscriptional activities, like protein binding and polyadenylation. Identifying SNPs associated with the development of complex disease is a significant pursuit in contemporary genetics studies.²⁴ With technologies that enable the analysis of hundreds of thousands of SNPs, along with insights into the structure of genomic variation in human genome,²⁵ it is possible to search for common genetic variations linked to disease risk. Several studies have successfully identified SNPs associated with vulnerability to diseases, such as breast cancer,²⁶ prostate cancer,²⁷ and type 2 diabetes.²⁸

To investigate the pathogenesis of PE, we conducted exome sequencing using the Human Exome BeadChip assays, and performed SNP screening using MassARRAY SNP genotyping on the peripheral blood of 370 sPE cases/482 healthy controls (HCs) and 498 sPE/500 HCs, respectively. After data analysis, we discovered that rs77133388 of *NSUN5* is significantly associated with an increased risk of PE. Using the CRISPR/Cas9 system, we created single-base mutant mice at rs77133388 in exon 7 of *NSUN5* to explore its role in the development of PE. Pregnant mice with the NSUN5 R295C mutation exhibited symptoms of PE that resulted from impairing decidualization through IL-11R α /JAK2/STAT3/Cyclin D3 pathway via direct binding of NSUN5 to IL-11R α . Our study offers insights into the PE pathogenesis and provides a solid foundation for the prevention and treatment of this disease.

RESULTS

The baseline clinical characteristics of the study population

The clinical characteristics of PE and HCs are shown in Table 1. There was no significant difference in maternal age between the PE and HC groups ($p > 0.05$). However, the systolic blood pressure and diastolic blood pressure of PE group were found significantly higher than those of HC group ($p < 0.05$), whereas the gestational age at delivery and the birth weight were significantly decreased in PE group ($p < 0.05$). In addition, proteinuria was not observed in women from the HC group.

Exome sequencing and MassARRAY SNP genotyping

DNA samples from 370 women with PE and 482 HCs were extracted and selected for Human Exome BeadChip assays. This analysis revealed 270241 SNPs. After preliminary screening, a total of 263039 SNP loci and 851 pregnant women (369 with sPE and 482 HCs) qualified for further analysis. Logistic regression was then performed to investigate the relationship between each SNP and sPE. Further screening of these SNPs in combination with their functions identified 21 promising susceptibility sites, including rs77133388 of *NSUN5*.²⁹ To validate rs77133388 of *NSUN5* and search for candidate genes, MassARRAY SNP genotyping was then performed on the *NSUN5* rs7713338846, along with 45 other promising SNPs associated with PE pathogenesis in the peripheral blood of pregnant women (498 with sPE and 500 with HCs). Genetic polymorphism analyses were then conducted, revealing that the polymorphisms of four SNPs among the 46 were significant in the sPE group compared to the HCs. The four significant SNP allelic frequencies were presented in Table 2. The data showed that the allele frequency of *NSUN5* rs77133388 differed significantly between sPE and HCs ($p < 0.05$, $OR = 1.748$, $95\%CI = 0.986-3.159$). Therefore, both exon sequencing and MassARRAY SNP genotyping screened and confirmed that *NSUN5* rs77133388 was significantly different in the peripheral blood of sPE patients compared to that of HCs. Consequently, *NSUN5* rs77133388 was selected for further study to determine its role in the occurrence and development of PE. The detection and screening strategies used to ultimately select *NSUN5* rs77133388 as the research subject are shown in Figure S1.

NSUN5 point mutation causes PE

To further understand the impact of this mutation on pregnancy-induced hypertension (PE), a mouse model, NSUN5 R295C, with a single base mutation was created using the CRISPR/Cas9 system. By microinjecting synthesized RNAs and single-strand oligodeoxynucleotide donor sequences into mouse zygotes, defined point mutation was introduced into the mouse genome, leading to the substitution of a single amino

Table 2. The analysis of the variants in the studied population cohorts

No.	GENE	SNP	GROUP	GENOTYPE	Allele frequency	Total	χ^2	p	OR AT 95%CI	
1	CYP2C9	rs1057910		A/C	7.82%		7.477	0.0043	2.003(1.208–3.383)	
				HCs	27	5.40%				500
				sPE	51	10.26%				497
2	EGLN3	rs1680695		G/T	35.29%		60.558	0.0005	1.647 (1.229–2.208)	
				HCs	159	33.13%				480
				sPE	171	37.58%				455
3	NSUN5	rs77133388		A/G	5.92%		4.023	0.0416	1.748 (0.986–3.159)	
				HCs	22	4.4%				500
				sPE	37	7.44%				497
4	PDK1	rs11904366		G/T	8.84%		17.062	3.66E-05	2.887 (1.697–5.033)	
				HCs	23	5.01%				459
				sPE	53	13.22%				401

Note: sPE, severe preeclampsia; HCs, Healthy controls; OR, odds ratio; 95%CI, 95%confidence interval.

acid in NSUN5 protein (see Figure S2.). Heterozygous NSUN5 R295C mice were obtained, and NSUN5 R295C homozygous mice were further obtained by hybridization between the heterozygous mice. Compared with non-pregnant NSUN5 R295C mice, pregnant NSUN5 R295C mice showed increased systolic blood pressure at embryo (E) 16.5 (Figure 1A), similar to late pregnancy hypertension in women with PE. However, diastolic blood pressure did not increase (Figure 1B). Proteinuria is a hallmark of PE, and the urinary protein (albumin/creatinine) levels in NSUN5 R295C mice increased at E18.5 (Figure 1C). Histological analysis revealed glomerular swelling in the kidneys of NSUN5 R295C mice at E18.5 (Figure 1D). Further analysis using electron microscopy revealed the presence of thickened basement membranes (red arrows) and shortened foot processes (black arrows) (Figure 1E). The thickness of the basement membranes (Figure 1F) was significantly elevated, whereas the length of the foot processes (Figure 1G) was significantly reduced. The pups and placentas at E18.5 are displayed in Figures 1H and 1I, respectively. The total litter weight (Figure 1J) and placental weight (Figure 1K) of NSUN5 R295C pregnant mice were reduced. These findings suggest that NSUN5 R295C pregnant mice exhibit PE symptoms.

NSun5 mutation inhibits decidualization and results in abnormal placental development

To investigate the cause of PE caused by NSUN5 mutation, we initially observed the morphological changes of the placenta by H&E staining. Compared to the placenta of wild type (WT) mice, the placentas of NSUN5 R295C mice were markedly smaller at E18.5 (Figure 2A). On further examination, we discovered that the smaller placentas had already formed by E14.5 (Figure 2B). According to the structure of the placenta, we measured and calculated three distinct regions of the placenta. Statistical analysis revealed that the total area of the placenta of NSUN5 R295C was significantly reduced at both E18.5 and E14.5 compared to that of WT mice (Figure 2C). Among these regions, only the decidual area of NSUN5 R295C was considerably reduced (Figure 2D), while the labyrinth area (Figure 2E) and the junctional zone area (Figure 2F) were unaffected. These findings suggest that NSUN5 R295C inhibits decidualization, hence leading to abnormal placental development.

Decidualization defects of NSUN5 R295C mice

To investigate abnormal placental development in NSUN5 R295C mice, we examined the decidualization status during embryonic development. We observed that compared to WT mice, the implantation sites were smaller in NSUN5 R295C mice (Figures 3A and 3B). H&E staining revealed a significant reduction in the number of polyploidy cells in NSUN5 R295C endometrium compared to WT mice during normal pregnancy (Figures 3C and 3D). To further explore the role of decidualization in placental development, we induced decidualization by intraluminal injection of sesame oil into the uteri of pseudopregnant WT and NSUN5 R295C mice at E3.5. We observed that the NSUN5 R295C uterus had a smaller deciduoma, which was pronounced in pseudopregnant WT mice at E7.5 (Figures 3E and 3F). In addition, during pseudopregnancy, the NSUN5 R295C mutation significantly reduced the number of polyploid cells induced by oil (Figures 3G and 3H). These findings suggest that the NSUN5 R295C mutation impairs decidualization and polyploidy.

NSUN5 R295C downregulates the expression level of Il-11 α

To further investigate the mechanism underlying impaired decidualization in NSUN5 R295C mice, RNA-seq was conducted using the deciduoma obtained from pseudopregnant WT and NSUN5 R295C uterus at E7.5. A total of 130 downregulated and 44 upregulated differentially expressed genes (DEGs) were identified, with a fold change cutoff of 0.585 (or $\log_2FC < -0.585$) and $FDR < 0.05$. The heatmap of the DEGs in NSUN5 R295C and WT mice is presented in Figure 4A. The DEGs were classified using the Gene ontology (GO) database based on the categories of biological processes (BP), cellular component (CC), and molecular function (MF). The top fifteen GO terms for the DEGs are

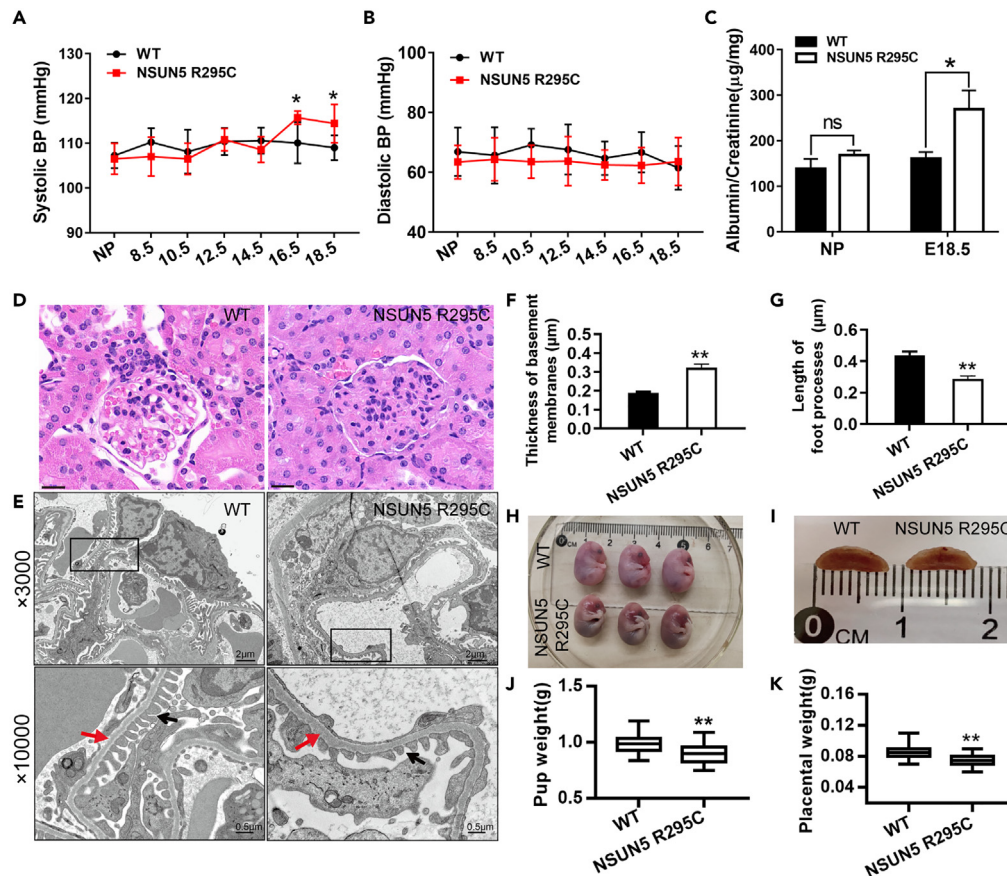


Figure 1. The mutation in *Nsun5* causes PE

(A) Changes in systolic blood and (B) diastolic blood pressure in NSUN5 R295C and wild type (WT) pregnant mice. For each genotype, $n = 7-11$. (C) Proteinuria measured by the urine albumin/creatinine ratios for pregnant NSUN5 R295C and WT mice at E18.5. For each genotype, $n = 6-9$. (D) Representative images of H & E-stained kidney sections of pregnant NSUN5 R295C and WT mice at E18.5 showing glomerular swelling. Scale bars: 20 μm . (E) Thickened glomerular basement membranes (red arrows) and shortened podocyte foot processes (black arrows) in NSUN5 R295C mice compared to WT at E18.5 under electron microscopy. The magnifications are 3,000 \times and 10,000 \times , respectively. Scale bars: 2 μm and 0.5 μm . The quantification of the thickness of basement membranes (F) and the length of foot processes (G). (H) Representative photos of the pup sizes at E18.5. (I) Representative photos of placenta sizes at E18.5. (J and K) The weight of individual pups (J) and placentas (K) are reduced in NSUN5 R295C mice compared to WT mice, respectively. For each genotype, $n = 8$. Data are represented as mean \pm SEM analyzed using the Student's *t* test, * $p < 0.05$, ** $p < 0.01$.

displayed in Figures 4B, S3A, and S3B. The dysregulated genes enriched in BP terms include the regulation of the immune system process and maternal process involved in female pregnancy. The DEGs are also presented as a volcano plot, which shows a significant downregulation in the expression level of *Il-11ra* (Figure 4C). This gene belongs to the BP of maternal process involved in female pregnancy (Figure 4B). The interleukin-11 receptor α chain (IL-11 α) is responsible for binding to IL-11, a pleiotropic cytokine belonging to the IL-6-type cytokine family. It signals through IL-11 α and signal transducers and activators of transcription (STAT) 3, and regulates cell cycle, invasion, and migration in various cell types.^{30,31} Kyoto Encyclopedia of Genes and Genomes (KEGG) pathway analysis was conducted to identify the potential biological functions of the significant DEGs. The results revealed fifteen signaling pathways, including hematopoietic cell lineage, ferroptosis, and Janus kinase and signal transducers and activators of transcription (JAK-STAT) signaling pathway, are associated with the downregulated DEGs (see Figure S3C). In the bubble pattern, the BP of maternal process involved in female pregnancy and JAK-STAT signaling pathway are also enriched (Figures S3D and S3E).

As identified from the previous results, IL-11 α is closely associated with defective decidualization. IL-11 α has previously been shown to be closely related to female reproduction, and IL-11 $\alpha^{-/-}$ mice are infertile due to decidualization defects.³² Therefore, IL-11 α was further studied. The expression of IL-11 α in deciduoma was then determined using immunohistochemistry at E7.5. The results showed that the IL-11 α level was significantly downregulated in the deciduoma of NSUN5 R295C mice compared with that of WT mice (Figures 4D and 4E). The mRNA level of *Il-11ra* was also significantly decreased in NSUN5 R295C mice (Figure 4F). The western blotting results indicated that the level of IL-11 α in the decidua of the NSUN5 R295C was also significantly reduced when compared to that of WT mice (Figures 4G and 4H). IL-11

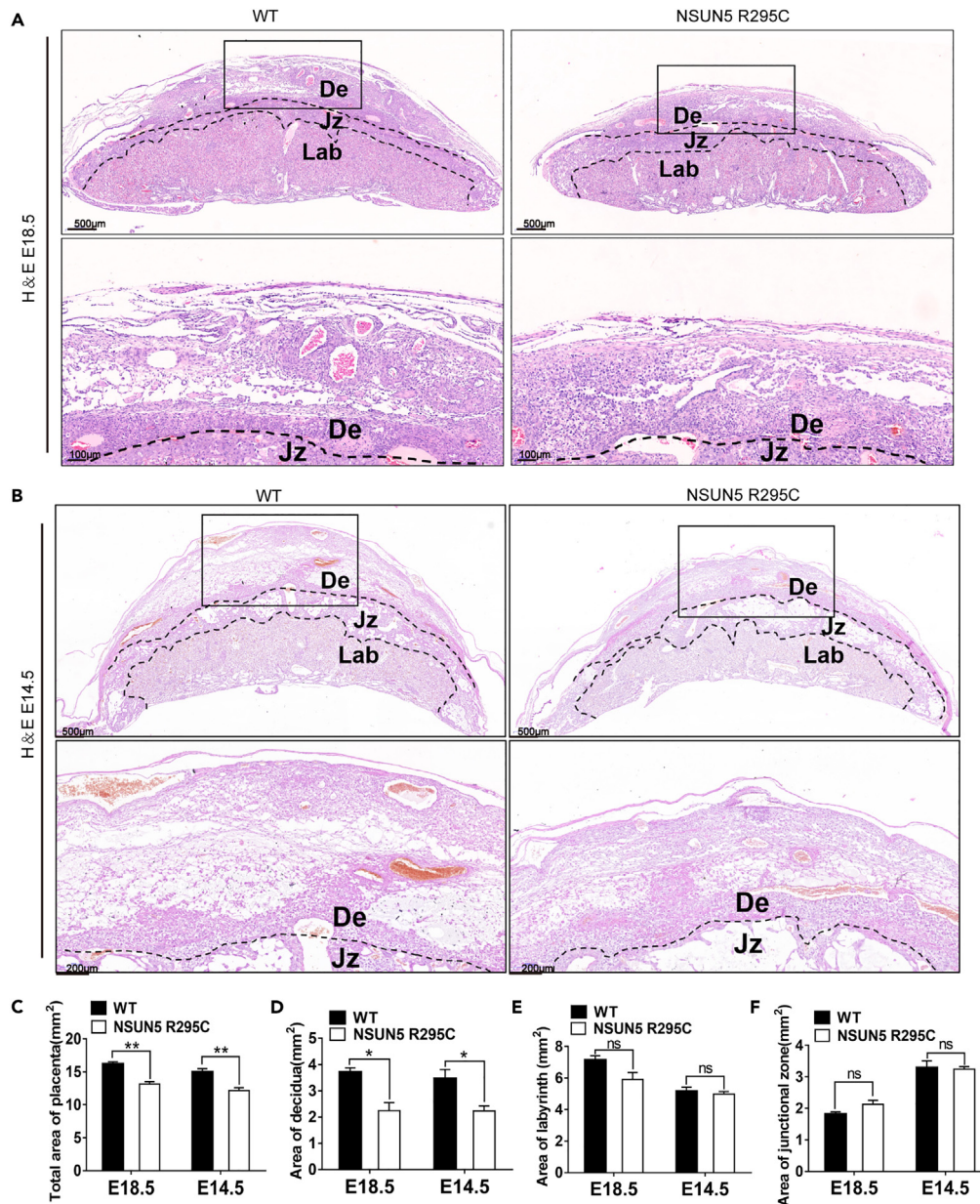


Figure 2. The mutation in *Nsun5* results in decidualization defects during pregnancy

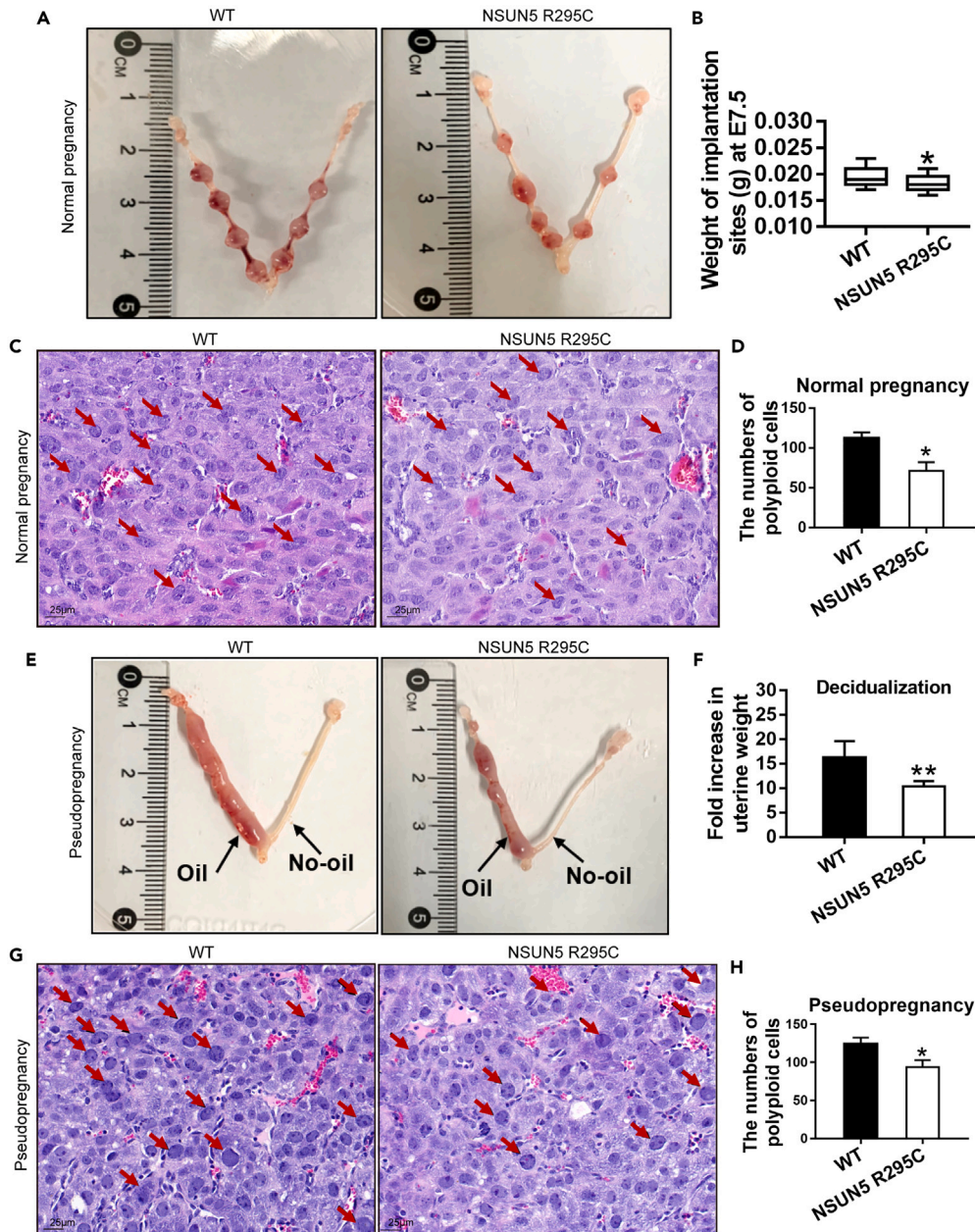
(A and B) Placental sections from WT and NSUN5 R295C embryos at E18.5 (A) and E14.5 (B) by H & E staining. Decidua: De; Labyrinth: Lab; Junctional zone: Jz. Scale bars: 500 μ m, 200 μ m, and 100 μ m.

(C–F) Reduced total placental area and decidual area in NSUN5 R295C mice at E18.5 and E14.5. The labyrinth area and junctional zone area are normal ($n = 6$ –9 per genotype). (C) Total placental area of WT and NSUN5 R295C embryos at E18.5 and E14.5. (D) The area of the decidua. (E) The area of the labyrinth. (F) The area of the junctional zone. Data are represented as mean \pm SEM analyzed using the Student's *t* test, * $p < 0.05$, ** $p < 0.01$.

signals through a heterodimer complex of IL-11R α and glycoprotein 130 (GP130).³³ Therefore, we also measured the mRNA and protein levels of GP130 and found that its expression remained unchanged (see Figure S4). These data suggest that the observed effect is attributed to a decrease in IL-11R α levels rather than a decrease in GP130 expression.

Downregulated Cyclin D3 caused by insufficient phosphorylation of JAK2 and STAT3 participates PE development

In the previous bioinformatics analysis and studies, it was observed that the DEGs were enriched in the JAK-STAT signaling pathway and that the expression levels of IL-11R α were significantly reduced in the deciduoma of NSUN5 R295C mice compared to that of WT mice. IL-11 triggers the



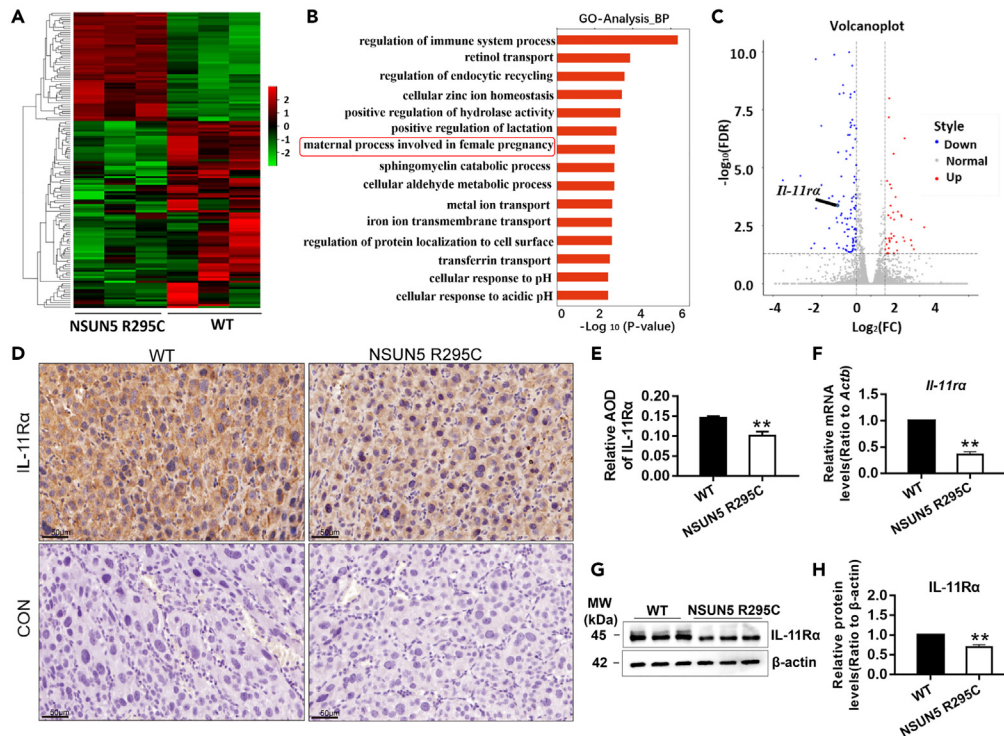


Figure 4. The mutation of *Nsun5* reduces *Il-11ra* expression

(A) The heatmap of global RNA-seq transcriptomic results revealed differentially expressed genes (DEGs) in the deciduoma obtained from pseudopregnant WT and NSUN5 R295C uterus at E7.5.
 (B) GO-BP analysis of the consistent DEGs. The top 15 enriched GO terms are shown in biological process (BP) with a $p < 0.05$.
 (C) Statistical significance ($-\log_{10}$ FDR) vs. gene expression \log_2 fold change (FC) is displayed as a volcano plot of global RNA-seq results. The label indicates: upregulated (red dots); downregulated (blue dots); not significant genes (gray dots).
 (D) Immunohistochemistry showed that the staining intensity of the IL-11R α positive cells is decreased in the deciduoma of pseudopregnant NSUN5 R295C mice compared to WT at E 7.5. Scale bar: 50 μ m.
 (E) The decidual tissue of pseudopregnant mice ($n = 5$ for each genotype) was photographed and examined. Average optical density (AOD) was used for the quantitative analysis of immunohistochemistry staining, and the data are shown in bar graphs.
 (F) The mRNA expression levels of *Il-11ra* in the decidua of NSUN5 R295C mice were lower than those in WT mice ($n = 8$ per genotype).
 (G) Results of western blotting showed that the protein level of IL-11R α was decreased in the decidua of NSUN5 R295C mice compared to those in WT.
 (H) The results of western blotting were quantified and displayed in bar graphs ($n = 6$ per genotype). Data are represented as mean \pm SEM analyzed using Student's *t* test. * $p < 0.05$; ** $p < 0.01$.

JAK-STAT signaling pathway by forming a heterodimer complex with glycoprotein 130 to induce cellular responses.³⁴ Additionally, Cyclin D3, a cell cycle regulator essential for decidual cell growth, is regulated by IL-11 signal.³⁵ Hence, to determine the role of IL-11R α in the progression of PE, the expression of JAK2, STAT3, Cyclin D3, and P21 in the deciduoma at E7.5 was investigated. The qPCR analysis revealed that the expression levels of *Cyclin D3* and *P21* were significantly reduced in the NSUN5 R295C mice, while the expression level of *Jak2* and *Stat3* remained unchanged (Figure 5A). Further, western blot analysis demonstrated that the phosphorylation levels of JAK2 and STAT3, as well as Cyclin D3 levels in the E7.5 deciduoma of NSUN5 R295C mice, were significantly downregulated (Figure 5B). Further, western blot analysis demonstrated that the phosphorylation levels of JAK2 and STAT3, as well as Cyclin D3 levels in the E7.5 deciduoma of NSUN5 R295C mice, were significantly downregulated (Figures 5C–5E). These findings suggest that Cyclin D3 expression in the decidua depends on IL-11 and JAK-STAT signaling.

To investigate the mechanism by which NSUN5 promotes PE, RIP was employed to identify its target transcripts. The results revealed that NSUN5 binds to *Il-11ra* mRNA in the deciduoma of pseudopregnant mice at E7.5 (Figures 5F and 5G), suggesting that *Il-11ra* is a potential target or substrate of NSUN5. Overall, these findings suggest that NSUN5 mutation leads to a reduction in IL-11R α , thereby downregulating the phosphorylation of JAK2 and STAT3. The subsequent insufficient activation of JAK2 and STAT3 inhibits Cyclin D3 expression and decidualization, eventually leading to the development of PE, as shown in Figure 5H.

DISCUSSION

In this study, we conducted exome sequencing using Human Exome BeadChip assays and gene analysis using MassARRAY SNP genotyping on the blood of 868 patients with sPE and 982 matched control subjects. We found that the SNP rs77133388 of *NSUN5* is significantly

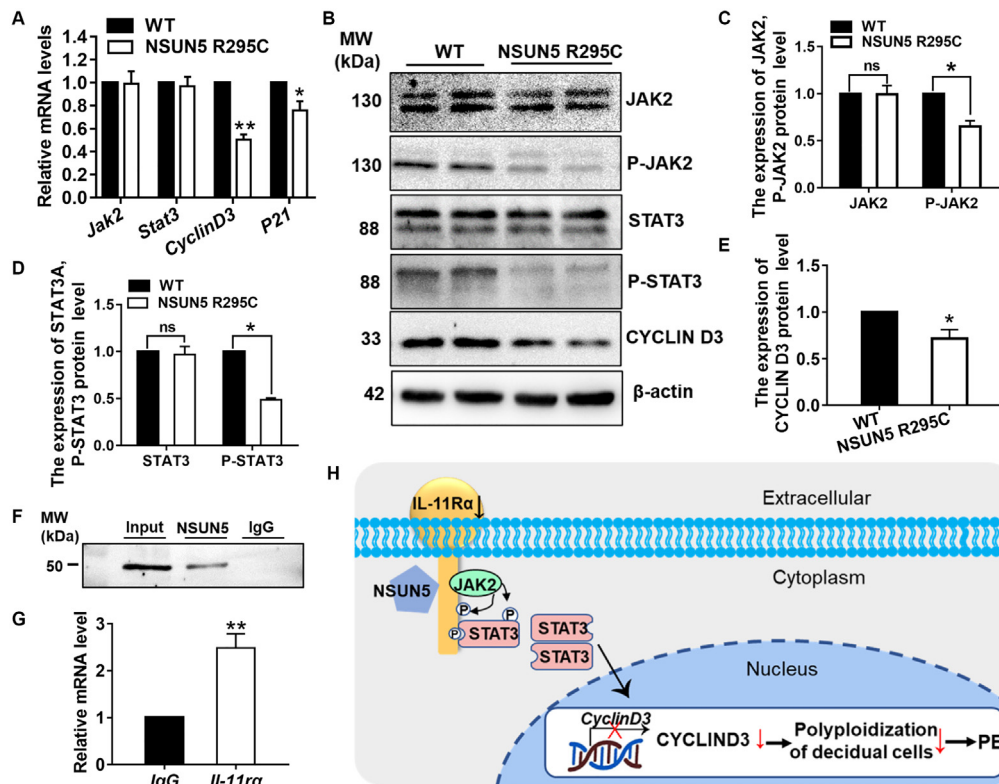


Figure 5. The mutation of *Nsun5* suppresses JAK/STAT signal pathway and downregulates Cyclin D3

(A) QPCR results showing the expressions of *Jak2*, *Stat3*, *Cyclin D3*, and *P21* in the decidua of NSUN5 R295C and WT mice at E7.5. (B) The expressions of JAK2, P-JAK2, STAT3, P-STAT3, and Cyclin D3 analyzed by western blot ($n = 6$ per genotype). The protein levels of P-JAK2, P-STAT3, and Cyclin D3 were decreased in the decidua of NSUN5 R295C mice when compared to those in WT mice. (C–E) The results of western blotting were quantified and shown in bar graphs. (C) The bar graphs show the relative density of P-JAK2 and JAK2 according to the statistical analysis of the results of three independently repeated experiments. (D) The bar graphs show the relative density of P-STAT3 and STAT3 according to the statistical analysis of the results of three independently repeated experiments. (E) The bar graph shows the relative density of Cyclin D3 according to statistical analysis of the results of three independently repeated experiments. (F and G) NSUN5 binds to *Il-11ra* mRNA in decidua as revealed by RNA immunoprecipitation (RIP). (H) Schematic diagram showing the mechanisms of NSUN5-IL-11R α interaction. NSUN5 mutation leads to IL-11R α down expression. Insufficient phosphorylation of JAK2 and STAT3 downregulates Cyclin D3, resulting in decreased polyploidization, and eventually leading to PE development. Data are represented as mean \pm SEM analyzed using Student's *t* test. * $p < 0.05$; ** $p < 0.01$.

associated with PE risk. Next, we generated single base mutant mice at rs77133388 in exon7 of *NSUN5*. Pregnant NSUN5 R295C mice showed typical symptoms of human PE, including hypertension, proteinuria, and reduced fetal and placental weight. Further study revealed that pregnant NSUN5 R295C mice had smaller placenta due to insufficient decidualization, while pseudopregnant NSUN5 R295C mice had a dramatically reduced number of polyploid cells at E7.5. Transcriptome analysis of the deciduoma at E7.5 uncovered that the DEGs were enriched in the JAK-STAT signaling pathway, and IL-11R α level was markedly decreased in NSUN5 R295C mice. Mechanism studies showed that decreased IL-11R α expression inhibits the activation of JAK2 and STAT3, which leads to reduced Cyclin D3 expression, subsequently, impairing the polyploidization of decidual cells, consequently contributing to the occurrence of PE.

PE, the primary cause of patient mortality, elevates the risk of chronic diseases in both mother and infant, significantly diminishing their quality of life.^{2,36} Nevertheless, the pathogenesis of PE currently remains unclear. Previous studies on the etiology of PE have largely concentrated on the placenta, including placental ischemia and dysfunction. However, the endometrium is the foundation of placentagenesis. Recently, an increasing number of studies have shown that abnormal decidualization constitutes a crucial factor in the development of PE.^{14,15,37–40} Several studies have detected impaired decidualization as the chief characteristic of PE, prompting shallow trophoblasts invasion.^{14,41} In addition, Garrido-Gomez et al. reported that the decidualization defects observed in patients with sPE at delivery persisted for years postpartum.¹⁴ In this study, we first investigated the role of NSUN5 in the pathogenesis of PE and discovered that a single base mutation, *NSUN5*rs77133388, is substantially correlated with PE. This mutation causes abnormal decidualization and thus contributes to the development of PE, presenting a perspective for studying the pathogenesis of PE.

NSUN5 belongs to the NOP2/Sun RNA methyltransferase (NSUN) protein family,⁴² several members of which have putative m⁵C methyltransferase activity. Some NSUN family proteins are associated with the regulation of protein translation, RNA processing, metabolism, and

cell differentiation.^{43–45} Studies have shown that NSUN2 and NSUN4 participate in cell proliferation and differentiation, and protein biosynthesis,⁴⁶ while NSUN3 regulates embryonic stem cell differentiation by promoting mitochondrial activity.⁴⁷ NSUN5 deficiency has been linked to a reduction in protein synthesis during mammalian development,¹⁸ and lack of *Nsun5* has been shown to inhibit ovarian function by decreasing the number of follicles.⁴⁸ However, it is not yet clear whether NSUN5 is involved in decidualization. Here, we reported that NSUN5 mutation results in insufficient decidualization and a reduced number of polyploid cells at E7.5. Previous studies have shown that polyploidization is a hallmark of mature decidual cells, and its attenuation during decidualization can lead to embryonic death before placentation.⁴⁹ Our results also suggested that polyploidization is critical for decidualization, and polyploidization deficiency leads to a flawed decidualization response. Moreover, our findings provide mechanistic insight into how NSUN5 mutation influences decidualization through the JAK2/STAT3 signaling pathway, which promotes the pathogenesis of PE.

In the present study, a comprehensive transcriptome analysis was conducted on deciduoma obtained from pseudopregnant WT and NSUN5 R295C uterus at E7.5. A total of 174 DEGs were identified, of which 44 genes were upregulated and 130 genes were downregulated. Further analysis of the DEGs using GO and KEGG showed a significant enrichment of BP in multiple biological processes. Additionally, the JAK-STAT signaling pathway was found to be significantly downregulated. Previous studies have supported our finding that signals mediated by IL-11R α are specifically required for normal female reproduction.⁵⁰ Evdokia Dimitriadis et al. have also demonstrated that targeted inhibition of IL-11R α impairs proliferation and invasion of human endometrial cancer cell *in vitro*.⁵¹ Moreover, studies have demonstrated that administering IL-11 to mice leads to the development of features similar to those seen in PE. IL-11 has been shown to increase the levels of pregnancy-associated plasma protein A2, which compromises trophoblastic invasion, spiral artery remodeling, and placentation.⁵² Leukemia inhibitory factor and IL-11 are essential regulators in the establishment of pregnancy.⁵³ Within cytokine families, there is evidence of pleiotropy, redundancy, and even duality, where multiple cytokines often possess similar, overlapping, and sometimes contrasting functions. Nevertheless, these discoveries indicate that the IL-11R α -JAK-STAT pathway may have a fundamental role to play.

IL-11 signals through IL-11R α and subsequently recruits GP130, ultimately resulting in the activation of the JAK/STAT pathway.⁵⁴ IL-11 is a cytokine that activates cells by binding to the IL-11R, and the presence of soluble IL-11R can mediate *trans*-signaling.⁵⁵ Christoph Garbers et al. analyzed prominent IL-11R mutations in patients and confirmed that they were detrimental to IL-11 signaling.⁵⁶ According to the findings of Lorraine et al., IL-11 and IL-11R α expression is prominent post-implantation, and in *IL-11R α ^{-/-}* mice, sterility can be attributed to defective decidualization.⁵⁷ Our research aligns with their findings, showing that the downregulation of IL-11R α rather than GP130 leads to the reduction in the expression level of P-JAK2, P-STAT3, Cyclin D3, and P21, resulting in impaired decidualization. Additionally, we demonstrated that NSUN5 binds to *IL-11R α* mRNA. Based on these findings, we concluded that NSUN5 mutation inhibits decidualization and contributes to the development of PE by regulating the JAK2/STAT3 signaling pathway.

In mammals, the JAK/STAT pathway serves as a major signaling mechanism for a various cytokines and growth factors. STATs get activated by tyrosine kinases belonging to the JAK family. Once activated, they dimerize and move to the nucleus, where they regulated the expression of specific genes. This orchestrating leads to hematopoiesis, inflammation induction, and immune response control.³⁴ Previous studies confirmed that changes in the JAK2/STAT3 pathway can impact the expression of cytokines such as TNF- α and IL-6,⁵⁸ and contributes to brain damage due to ischemia/reperfusion.⁵⁹ Our research shows that inhibiting JAK2/STAT3 pathway can restrict decidualization by reducing Cyclin D3, resulting in the development of PE. It is known that P-STAT3 translocates to the nucleus and directly regulates the transcription of target genes by binding to DNA. Previous reports have indicated that Cyclin D3 promotes the development of polyploidy during stromal cell decidualization.^{35,60,61}

Our finding carries significant clinical implication as they shed light on the crucial role of NSUN5 R295C in decidual dysfunction. It is worth noting that this mutation validates the clinical relevance of the model as there is a significant difference in the genotypic and allelic frequencies of *NSUN5* SNP rs77133388 in cases and controls from clinical data. We utilized the CRISPR/Cas9 system⁶² to create a single amino acid substituted mouse model that resulted in single amino acid substitutions in the proteins of interest. This technique facilitates the elucidation of *in vivo* contexts of findings in cultured cell systems, and *in vivo* screening for the relevant mutations found in human patients with various diseases.⁶³ Impaired NSUN5 expression or function in the pregnant decidual tissue represents an important mechanism underlying PE. We carefully select suitable methods to test decidualization, including artificially induced decidualization, histological analysis, microscopy and imaging, as well as functional assays. By employing these methods, we are capable of evaluating the extent of decidualization from various perspectives and levels, and understanding the influence of decidualization on PE, both with and without embryos. Further investigations to understand impaired decidual NSUN5 expression in PE patients may aid in developing strategies to enhance the NSUN5/IL-11R α /JAK/STAT pathway and treat this life-threatening disease.

Limitations of the study

This study has some limitations. Firstly, in order to address potential overfitting issues that may arise from analyzing a single dataset in the modeling process, we employed several strategies. These included making efforts to obtain a larger number of samples for training and reducing model complexity by utilizing multivariate logistic regression analysis. However, it is important to note that completely preventing model overfitting can be challenging. Secondly, it is currently unknown whether the m⁵C modification of NSUN5 plays a role in regulating decidual genes during the development of PE. Lastly, the regulation of IL-11 and IL-11R α production appears to be complex and likely dependent on tightly regulated local microenvironments, as well as the interplay between individual positive and negative regulators. Therefore, conducting large-scale clinical trials is necessary to further investigate the relationship between rs77133388 of *NSUN5* and the occurrence of PE, as well as to determine the precise underlying mechanism.

STAR★METHODS

Detailed methods are provided in the online version of this paper and include the following:

- **KEY RESOURCES TABLE**
- **RESOURCE AVAILABILITY**
 - Lead contact
 - Materials availability
 - Data and code availability
- **EXPERIMENTAL MODEL AND STUDY PARTICIPANT DETAILS**
 - Mice
 - Human subject
- **METHOD DETAILS**
 - Exome sequencing and SNP selection
 - MassARRAY SNP genotyping and data analysis
 - Mouse biometric measurements
 - Transmission electron microscopy (TEM)
 - Artificially induced decidualization
 - RNA sequencing (RNA-Seq) and data analysis
 - Histological analysis and immunohistochemistry
 - Quantitative polymerase chain reaction (qPCR) analysis
 - Western blot
 - RNA immunoprecipitation (RIP) assay
- **QUANTIFICATION AND STATISTICAL ANALYSIS**

SUPPLEMENTAL INFORMATION

Supplemental information can be found online at <https://doi.org/10.1016/j.isci.2024.108899>.

ACKNOWLEDGMENTS

This study was supported by the National Key R&D Program of China (2019YFA0802600) and the National Natural Science Foundation of China (32170863 and 31871512) to C.Z. Support was also received from grants from the Shanghai Commission of Science and Technology (20DZ2270900) and Open Project of Shandong Provincial Key Laboratory of Reproductive Medicine (SDKL2017018). We are grateful to Yan-Ling Wang (Institute of Zoology, Chinese Academy of Sciences) for their contribution to the partial SNP screening.

AUTHOR CONTRIBUTIONS

Conceptualization, H.Z., H.L., and C.Z.; methodology, J.Y. and M.Z.; investigation, H.L., J.Y., and M.Z.; writing – original draft, H.Z. and M.Z.; writing – review and editing, H.Z. and C.Z.; funding acquisition, C.Z.

DECLARATION OF INTERESTS

The authors declare no competing interests.

Received: September 10, 2023

Revised: November 24, 2023

Accepted: January 9, 2024

Published: January 31, 2024

REFERENCES

1. Rich-Edwards, J.W., Fraser, A., Lawlor, D.A., and Catov, J.M. (2014). Pregnancy characteristics and women's future cardiovascular health: an underused opportunity to improve women's health? *Epidemiol. Rev.* 36, 57–70.
2. Burton, G.J., Redman, C.W., Roberts, J.M., and Moffett, A. (2019). Pre-eclampsia: pathophysiology and clinical implications. *BMJ* 366, l2381.
3. Magee, L.A., Nicolaidis, K.H., and von Dadelszen, P. (2022). Preeclampsia. *N Engl J Med* 386, 1817–1832.
4. Sones, J.L., and Davison, R.L. (2016). Preeclampsia, of mice and women. *Physiol. Genom.* 48, 565–572.
5. Tong, J., Lv, S., Yang, J., Li, H., Li, W., and Zhang, C. (2022). Decidualization and Related Pregnancy Complications. *Maternal-Fetal Medicine* 4, 24–35.
6. Mol, B.W.J., Roberts, C.T., Thangaratinam, S., Magee, L.A., de Groot, C.J.M., and Hofmeyr, G.J. (2016). Pre-eclampsia. *Lancet* 387, 999–1011.
7. Redman, C. (2014). The six stages of pre-eclampsia. *Pregnancy Hypertens* 4, 246.
8. Gathiram, P., and Moodley, J. (2020). The Role of the Renin-Angiotensin-Aldosterone System in Preeclampsia: a Review. *Curr. Hypertens. Rep.* 22, 89.
9. Hiby, S.E., Walker, J.J., O'Shaughnessy K, M., Redman, C.W., Carrington, M., Trowsdale, J., and Moffett, A. (2004). Combinations of maternal KIR and fetal HLA-C genes influence the risk of preeclampsia and reproductive success. *J. Exp. Med.* 200, 957–965.

10. Cui, Y., Wang, W., Dong, N., Lou, J., Srinivasan, D.K., Cheng, W., Huang, X., Liu, M., Fang, C., Peng, J., et al. (2012). Role of corin in trophoblast invasion and uterine spiral artery remodelling in pregnancy. *Nature* **484**, 246–250.
11. Zhu, Y.-Q., Yan, X.-Y., Li, H., and Zhang, C. (2021). Insights into the Pathogenesis of Preeclampsia Based on the Features of Placentation and Tumorigenesis. *Reproductive and Developmental Medicine* **5**, 97–106.
12. Carolyn, L., and Dunn, R.W.K. (2003). Decidualization of the human endometrial stromal cell: an enigmatic transformation. *Reproductive BioMedicine* **No 2**, 151–161.
13. Zhang, C., Large, M.J., Duggavathi, R., DeMayo, F.J., Lydon, J.P., Schoonjans, K., Kovanci, E., and Murphy, B.D. (2013). Liver receptor homolog-1 is essential for pregnancy. *Nat. Med.* **19**, 1061–1066.
14. Garrido-Gomez, T., Dominguez, F., Quinonero, A., Diaz-Gimeno, P., Kapidzic, M., Gormley, M., Ona, K., Padilla-Iserte, P., McMaster, M., Genbacev, O., et al. (2017). Defective decidualization during and after severe preeclampsia reveals a possible maternal contribution to the etiology. *Proc. Natl. Acad. Sci. USA* **114**, E8468–E8477.
15. Garrido-Gomez, T., Quinonero, A., Dominguez, F., Rubert, L., Perales, A., Hajjar, K.A., and Simon, C. (2020). Preeclampsia: a defect in decidualization is associated with deficiency of Annexin A2. *Am. J. Obstet. Gynecol.* **222**, 376.e1–e17.
16. Wang, G., Zhang, Z., Chen, C., Zhang, Y., and Zhang, C. (2016). Dysfunction of WNT4/WNT5A in deciduas: possible relevance to the pathogenesis of preeclampsia. *J. Hypertens.* **34**, 719–727.
17. Lv, H., Tong, J., Yang, J., Lv, S., Li, W.P., Zhang, C., and Chen, Z.J. (2018). Dysregulated Pseudogene HK2P1 May Contribute to Preeclampsia as a Competing Endogenous RNA for Hexokinase 2 by Impairing Decidualization. *Hypertension* **71**, 648–658.
18. Heissenberger, C., Liendl, L., Nagelreiter, F., Gonskikh, Y., Yang, G., Stelzer, E.M., Krammer, T.L., Micutkova, L., Vogt, S., Kreil, D.P., et al. (2019). Loss of the ribosomal RNA methyltransferase NSUN5 impairs global protein synthesis and normal growth. *Nucleic Acids Res.* **47**, 11807–11825.
19. Jiang, Z., Li, S., Han, M.-J., Hu, G.-M., and Cheng, P. (2020). High expression of NSUN5 promotes cell proliferation via cell cycle regulation in colorectal cancer. *Am J Transl Res* **12**, 3858–3870.
20. Wang, Y., Jiang, T., Xu, J., Gu, Y., Zhou, Y., Lin, Y., Wu, Y., Li, W., Wang, C., Shen, B., et al. (2021). Mutations in RNA Methyltransferase Gene NSUN5 Confer High Risk of Outflow Tract Malformation. *Front. Cell Dev. Biol.* **9**, 623394.
21. Yuan, Z., Chen, P., Zhang, T., Shen, B., and Chen, L. (2019). Agnesis and Hypomyelination of Corpus Callosum in Mice Lacking Nsun5, an RNA Methyltransferase. *Cells* **8**.
22. Liu, J., Ren, Z., Yang, L., Zhu, L., Li, Y., Bie, C., Liu, H., Ji, Y., Chen, D., Zhu, M., and Kuang, W. (2022). The NSUN5-FTH1/FTL pathway mediates ferroptosis in bone marrow-derived mesenchymal stem cells. *Cell Death Dis.* **8**, 99.
23. Chen, P.-Y.K.X. (2003). Detection of Single Nucleotide Polymorphisms. *Curr. Issues Mol. Biol.* **5**, 43–60.
24. Wu, M.C., Kraft, P., Epstein, M.P., Taylor, D.M., Chanock, S.J., Hunter, D.J., and Lin, X. (2010). Powerful SNP-set analysis for case-control genome-wide association studies. *Am. J. Hum. Genet.* **86**, 929–942.
25. Hirschhorn, J.N., and Daly, M.J. (2005). Genome-wide association studies for common diseases and complex traits. *Nat. Rev. Genet.* **6**, 95–108.
26. Hunter, D.J., Kraft, P., Jacobs, K.B., Cox, D.G., Yeager, M., Hankinson, S.E., Wacholder, S., Wang, Z., Welch, R., Hutchinson, A., et al. (2007). A genome-wide association study identifies risk alleles in FGFR2 associated with risk of sporadic postmenopausal breast cancer. *Nat. Genet.* **39**, 870–874.
27. Gudmundsson, J., Sulem, P., Manolescu, A., Amundadottir, L.T., Gudbjartsson, D., Helgason, A., Rafnar, T., Bergthorsson, J.T., Agnarsson, B.A., Baker, A., et al. (2007). Genome-wide association study identifies a second prostate cancer susceptibility variant at 8q24. *Nat. Genet.* **39**, 631–637.
28. Scott, L.J., Mohlke, K.L., Bonnycastle, L.L., Willer, C.J., Li, Y., Duran, W.L., Erdos, M.R., Stringham, H.M., Chines, P.S., Jackson, A.U., et al. (2007). A genome-wide association study of type 2 diabetes in Finns detects multiple susceptibility variants. *Science* **316**, 1341–1345.
29. Li, H., Yan, X., Yang, M., Liu, M., Tian, S., Yu, M., Li, W.-P., Zhang, C., and Moreira, T.M.M. (2021). The Impact of PTPRK and ROS1 Polymorphisms on the Preeclampsia Risk in Han Chinese Women. *Int. J. Hypertens.* **2021**, 1–10.
30. Paul, S.R. (1990). Molecular cloning of a cDNA encoding interleukin 11, a stromal cell-derived lymphopoietic and hematopoietic cytokine. *Proc. Natl. Acad. Sci. USA* **87**, 7512–7516.
31. Salamonsen, L.A., Tan, Y.-L., Stoikos, C., and Dimitriadis, E. (2006). Interleukin 11 Signaling Components Signal Transducer and Activator of Transcription 3 (STAT3) and Suppressor of Cytokine Signaling 3 (SOCS3) Regulate Human Endometrial Stromal Cell Differentiation. *Endocrinology* **147**, 3809–3817.
32. Petra Bilinski, D.R., and Gossler, A. (1998). Maternal IL-11R α Function Is Required for Normal Decidua and Fetoplacental Development in Mice (GENES & DEVELOPMENT).
33. Du, X., W.D. (1997). Interleukin-11: review of molecular, cell biology, and clinical use. *Blood* **89**, 3897–3908.
34. Morris, R., Kershaw, N.J., and Babon, J.J. (2018). The molecular details of cytokine signaling via the JAK/STAT pathway. *Protein Sci.* **27**, 1984–2009.
35. Li, F., Devi, Y.S., Bao, L., Mao, J., and Gibori, G. (2008). Involvement of cyclin D3, CDKN1A (p21), and BIRC5 (Survivin) in interleukin 11 stimulation of decidualization in mice. *Biol. Reprod.* **78**, 127–133.
36. Irgens HU, R.L., Irgens, L.M., and Lie, R.T. (2001). Long term mortality of mothers and fathers after pre-eclampsia: population based cohort study. *BMJ* **323**, 1213–1217.
37. Franco, H.L., Dai, D., Lee, K.Y., Rubel, C.A., Roop, D., Boerboom, D., Jeong, J.W., Lydon, J.P., Bagchi, I.C., Bagchi, M.K., and DeMayo, F.J. (2011). WNT4 is a key regulator of normal postnatal uterine development and progesterone signaling during embryo implantation and decidualization in the mouse. *Faseb. J.* **25**, 1176–1187.
38. Wang, Q., Lu, J., Zhang, S., Wang, S., Wang, W., Wang, B., Wang, F., Chen, Q., Duan, E., Leitges, M., et al. (2013). Wnt6 is essential for stromal cell proliferation during decidualization in mice. *Biol. Reprod.* **88**, 5.
39. Garrido-Gomez, T., Castillo-Marco, N., Cordero, T., and Simon, C. (2020). Decidualization resistance in the origin of preeclampsia. *Am. J. Obstet. Gynecol.* **226**, S886–S894.
40. Yang, M., Li, H., Rong, M., Zhang, H., Hou, L., and Zhang, C. (2022). Dysregulated GLUT1 may be involved in the pathogenesis of preeclampsia by impairing decidualization. *Mol. Cell. Endocrinol.* **540**, 111509.
41. Lockwood, C.J., Basar, M., Kayisli, U.A., Guzeloglu-Kayisli, O., Murk, W., Wang, J., De Paz, N., Shapiro, J.P., Masch, R.J., Semerci, N., et al. (2014). Interferon-gamma protects first-trimester decidual cells against aberrant matrix metalloproteinases 1, 3, and 9 expression in preeclampsia. *Am. J. Pathol.* **184**, 2549–2559.
42. Zhang, T., Chen, P., Li, W., Sha, S., Wang, Y., Yuan, Z., Shen, B., and Chen, L. (2019). Cognitive deficits in mice lacking Nsun5, a cytosine-5 RNA methyltransferase, with impairment of oligodendrocyte precursor cells. *Glia* **67**, 688–702.
43. Meyer, K.D., and Jaffrey, S.R. (2014). The dynamic epitranscriptome: N6-methyladenosine and gene expression control. *Nat. Rev. Mol. Cell Biol.* **15**, 313–326.
44. Squires, J.E., Patel, H.R., Nousch, M., Sibbritt, T., Humphreys, D.T., Parker, B.J., Suter, C.M., and Preiss, T. (2012). Widespread occurrence of 5-methylcytosine in human coding and non-coding RNA. *Nucleic Acids Res.* **40**, 5023–5033.
45. Yang, X., Yang, Y., Sun, B.F., Chen, Y.S., Xu, J.W., Lai, W.Y., Li, A., Wang, X., Bhattarai, D.P., Xiao, W., et al. (2017). 5-methylcytosine promotes mRNA export - NSUN2 as the methyltransferase and ALYREF as an m(5)C reader. *Cell Res.* **27**, 606–625.
46. Sun, Z., Xue, S., Zhang, M., Xu, H., Hu, X., Chen, S., Liu, Y., Guo, M., and Cui, H. (2020). Aberrant NSUN2-mediated m(5)C modification of H19 lncRNA is associated with poor differentiation of hepatocellular carcinoma. *Oncogene* **39**, 6906–6919.
47. Trixl, L., Amort, T., Wille, A., Zinni, M., Ebner, S., Hechenberger, C., Eichen, F., Gabriel, H., Schoberleitner, I., Huang, A., et al. (2018). RNA cytosine methyltransferase Nsun3 regulates embryonic stem cell differentiation by promoting mitochondrial activity. *Cell. Mol. Life Sci.* **75**, 1483–1497.
48. Ding, C., Lu, J., Li, J., Hu, X., Liu, Z., Su, H., Li, H., and Huang, B. (2022). RNA-methyltransferase Nsun5 controls the maternal-to-zygotic transition by regulating maternal mRNA stability. *Clin. Transl. Med.* **12**, e1137.
49. Mori, M., Kitazume, M., Ose, R., Kurokawa, J., Koga, K., Osuga, Y., Arai, S., and Miyazaki, T. (2011). Death effector domain-containing protein (DEDD) is required for uterine decidualization during early pregnancy in mice. *J. Clin. Invest.* **121**, 318–327.
50. Petra Bilinski, D.R., and Gossler, A. (1998). Maternal IL-11R α function is required for normal decidua and fetoplacental development in mice. *GENES & DEVELOPMENT* **12**, 2234–2243.
51. Winship, A.L., Van Sinderen, M., Donoghue, J., Rainczuk, K., and Dimitriadis, E. (2016). Targeting Interleukin-11 Receptor- α Impairs Human Endometrial Cancer Cell Proliferation

- and Invasion In Vitro and Reduces Tumor Growth and Metastasis In Vivo. *Mol. Cancer Therapeut.* 15, 720–730.
52. Winship, A.L., Koga, K., Menkhorst, E., Van Sinderen, M., Rainczuk, K., Nagai, M., Cuman, C., Yap, J., Zhang, J.-G., Simmons, D., et al. (2015). Interleukin-11 alters placentation and causes preeclampsia features in mice. *Proc. Natl. Acad. Sci. USA* 112, 15928–15933.
 53. Paiva, P., Menkhorst, E., Salamonsen, L., and Dimitriadis, E. (2009). Leukemia inhibitory factor and interleukin-11: Critical regulators in the establishment of pregnancy. *Cytokine Growth Factor Rev.* 20, 319–328.
 54. Du, X., and Williams, D.A. (1997). Interleukin-11: Review of Molecular, Cell Biology, and Clinical Use. *Blood* 89, 3897–3908.
 55. Lokau, J., Agthe, M., and Garbers, C. (2016). Generation of Soluble Interleukin-11 and Interleukin-6 Receptors: A Crucial Function for Proteases during Inflammation. *Mediat. Inflamm.* 2016, 1–10.
 56. Agthe, M., Brügge, J., Garbers, Y., Wandel, M., Kespohl, B., Arnold, P., Flynn, C.M., Lokau, J., Aparicio-Siegmund, S., Bretscher, C., et al. (2018). Mutations in Craniosynostosis Patients Cause Defective Interleukin-11 Receptor Maturation and Drive Craniosynostosis-like Disease in Mice. *Cell Rep.* 25, 10–18.e15.
 57. Lorraine Robb, R.L., and Lynne, H. (1998). Infertility in female mice lacking the receptor for interleukin 11 is due to a defective uterine response to implantation. *Nat. Med.* 4, 303–308.
 58. Liu, C., Zhao, Q., Zhong, L., Li, Q., Li, R., Li, S., Li, Y., Li, N., Su, J., Dhondrup, W., et al. (2021). Tibetan medicine Ershiwuwei Lvxue Pill attenuates collagen-induced arthritis via inhibition of JAK2/STAT3 signaling pathway. *J. Ethnopharmacol.* 270, 113820.
 59. Hu, G.Q., Du, X., Li, Y.J., Gao, X.Q., Chen, B.Q., and Yu, L. (2017). Inhibition of cerebral ischemia/reperfusion injury-induced apoptosis: nicotiflorin and JAK2/STAT3 pathway. *Neural Regen Res* 12, 96–102.
 60. Das, S.K., Lim, H., and Paria, B.C. (1999). Cyclin D3 in the mouse uterus is associated with the decidualization process during early pregnancy. *J. Mol. Endocrinol.* 91–101.
 61. Das, S.K. (2002). Evidence for coordinated interaction of cyclin D3 with p21 and cdk6 in directing the development of uterine stromal cell decidualization and polyploidy during implantation. *Mech. Dev.* 111, 99–113.
 62. Hryhorowicz, M., Lipinski, D., Zeyland, J., and Slomski, R. (2017). CRISPR/Cas9 Immune System as a Tool for Genome Engineering. *Arch. Immunol. Ther. Exp.* 65, 233–240.
 63. Inui, M., Miyado, M., Igarashi, M., Tamano, M., Kubo, A., Yamashita, S., Asahara, H., Fukami, M., and Takada, S. (2014). Rapid generation of mouse models with defined point mutations by the CRISPR/Cas9 system. *Sci. Rep.* 4, 5396.
 64. Lena Ho, M.V.D., and Bruno, R. (2017). ELABELA deficiency promotes preeclampsia and cardiovascular malformations in mice. *Science* 355, 1126.
 65. Cui, L.L., Yang, G., Pan, J., and Zhang, C. (2011). Tumor necrosis factor alpha knockout increases fertility of mice. *Theriogenology* 75, 867–876.
 66. Kim, D., Langmead, B., and Salzberg, S.L. (2015). HISAT: a fast spliced aligner with low memory requirements. *Nat. Methods* 12, 357–360.
 67. Falcon, S., and Gentleman, R. (2007). Using GOstats to test gene lists for GO term association. *Bioinformatics* 23, 257–258.

STAR★METHODS

KEY RESOURCES TABLE

REAGENT or RESOURCE	SOURCE	IDENTIFIER
Antibodies		
Anti-IL-11R α Antibody	HuaBio	Cat. NO: HA600056; Lot.: HO0702
IL6ST Rabbit pAb	ABclonal	Cat. NO: A18036; RRID: AB_2861832
NSUN5 Polyclonal Antibody	Thermo Fisher	PA5-54228; RRID: AB_2644824
JAK2 Rabbit pAb	ABclonal	Cat. NO: A19629; RRID: AB_2862706
Phospho-JAK2-Y1007 Rabbit pAb	ABclonal	Cat. NO: Ap0917; RRID: AB_2863830
STAT3 Rabbit mAb	ABclonal	Cat. NO: A19566; RRID: AB_2862671
Phospho- STAT3-Y705 Rabbit mAb	ABclonal	Cat. NO: AP0705; RRID: AB_2863810
Anti-Cyclin D3 Antibody	HuaBio	Cat:ET1612-4; RRID: AB_3070113
Rabbit monoclonal antibody Anti-actin	HuaBio	Cat:ET1701-80; RRID: AB_2943481
Antibody Anti-Rabbit IgG	HuaBio	Cat: HA1002; Lot: HL0421
Goat anti-Rabbit IgG HRP	HuaBio	Cat: HA1001; RRID: AB_2819166
Critical commercial assays		
Mouse Albumin ELISA Kit	Sigma-Aldrich	E99-134; RRID: AB_2892029
Creatinine (urinary)Colorimetric Assay Kit	Cayman Chemical	Item:500701; Batch:0584517
RNA Immunoprecipitation Kit	Geneseed	Cat#: P0101; Lot#: 20220606-015
Deposited data		
Mouse decuduoma RNA-seq	This paper	GEO: GSE249593
Experimental models: Organisms/strains		
C57BL/6 mice	Shandong normal university	NA
Software and algorithms		
Illumina Genome Studio software	Illumina	V2011
Agena Bioscience Assay Design Suite	Agena Bioscience	version 3.1
MassARRAY Typer 4.0 software	Agena Bioscience	Typer 4.0

RESOURCE AVAILABILITY

Lead contact

Further information and requests for resources and reagents should be directed to and will be fulfilled by the lead contact, Dr. Cong Zhang (zhangxinyunlife@163.com)

Materials availability

This study did not generate new unique reagents.

Data and code availability

- The data have been deposited at the NCBI Gene Expression Omnibus (GEO) repository and are publicly available as of the date of publication. Accession numbers are listed in the [key resources table](#).
- This study does not report original code.
- Any additional information required to reanalyze the data reported in this paper is available from the [lead contact](#) upon request.

EXPERIMENTAL MODEL AND STUDY PARTICIPANT DETAILS

Mice

The *NSUN5* (R295C) mutation was introduced into mice using CRISPR-Cas9 techniques. The Cas9-guide RNA (gRNA) target sequences were designed to the intron7 regions to facilitate DNA breaks and homologous recombination. The *in vitro* transcribed nuclease Cas9 mRNA, gRNA, and the oligo donor carrying the desired mutation (CGT→TGT, R295→C295) were co-injected into fertilized mouse eggs of C57BL/6 background and transplanted into the oviducts of recipient mice. The pups were identified through PCR followed by sequence analysis using primers (*NSUN5* R295C-F: GACTCACAACCTGTTCTATCT; *NSUN5* R295C-R: GGCATCTCCAGTATCCAAG). Each reaction mix contained 12.5μL of 2X buffer, 1μL of primer mix, 5μL of dNTP, 0.5μL of KOD FX, 2μL of DNA template, and 4μL of ddH₂O. The PCR conditions were set as follows conditions: initial denaturation at 94°C for 2 min, 35 cycles of 98°C for 10s, 60°C for 30s, and 68°C for 20s, followed by a final extension at 68°C for 10 min. The mice were housed in the Animal Center of Shandong Normal University at 23±2°C and provided *ad libitum* access to food and water under a 12/12h light/dark cycle. We selected adult male and female mice with a C57BL/6J genetic background for co-breeding. Then pregnant female mice were chosen for the experiment. All animal experiments were carried out in compliance with the Guidelines for the Care and Use of Laboratory Animals of Shandong Normal University and were authorized by the Animal Ethics Committee of Shandong Normal University.

Human subject

A total of 482 individuals with healthy pregnancies, matched in age and gestational week, were recruited alongside 370 individuals with sPE for exome sequencing using Human Exome BeadChip assays. Following exome sequencing, 500 HCs and 498 individuals with sPE were selected for SNP screening using MassARRAY SNP Genotyping assays. All the pregnant women were Han Chinese women between the ages of 18 and 45. A normal pregnancy was defined as a pregnancy resulting in a healthy newborn delivered at term (>37 weeks of gestation) with normal blood pressure and no complications. The sPE was defined as a PE patient with systolic blood pressure ≥ 160 mm Hg and/or diastolic blood pressure ≥ 110 mm Hg, with or without proteinuria. Exclusion criteria included major fetal chromosomal or congenital abnormalities, autoimmune diseases, chronic hypertension, cardiovascular and metabolic diseases, multiparous pregnancies, stillbirth, and renal diseases. All samples were collected from the Provincial Hospital Affiliated to Shandong University, the First Affiliated Hospital of Nanjing Medical University, and the Second Affiliated Hospital of Nanjing Medical University between December 2009 and February 2015. Written informed consent was obtained from all participants at recruitment, and the study was approved by the relevant ethics committees.

METHOD DETAILS

Exome sequencing and SNP selection

In previous study, we extracted DNA samples from 370 sPE cases and 482 HCs from peripheral blood using Wizard® Genomic DNA Purification Kit (Promega Biotech Co., Ltd, Beijing, China), following the manufacturer's protocol as previously reported.²⁹ The Human Exome BeadChip (Illumina, San Diego, California, USA) was then utilized to assay the intact genomic DNA. By reading the raw data of the chip scanning through Illumina Genome Studio software (V2011), age-adjusted multivariable logistic regression analysis was conducted to identify SNPs with a significant association with PE by obtaining a *P*-value of <0.05.²⁹ We combined the functions of the SNPs and identified 21 susceptibility genes through data analysis,²⁹ which includes *NSUN5* rs77133388.

MassARRAY SNP genotyping and data analysis

To validate candidate genes, we conducted MassARRAY SNP genotyping to screen 46 promising SNPs (including *NSUN5* rs77133388) in the peripheral blood of pregnant women (498 sPE/500 HCs). The amplification and extension primers were designed using Agena Bioscience Assay Design Suite version 3.1 (Agena Bioscience, San Diego, California, USA). Primary multiplex PCRs were run on a GeneAmp 9700 PCR machine (Applied Biosystems, Carlsbad, California, USA). Each reaction mix contained 0.5μL of 10×PCR buffer, 1μL of primer mix, 0.4μL of MgCl₂, 0.1μL of dNTP, 0.2μL of Hotstar, and 20 ng of DNA template. The PCR conditions were set as follows: initial denaturation at 94°C for 4 min; 45 cycles of 94°C for 20s, 56°C for 30s, and 72°C for 60s; followed by a final extension at 72°C for 3 min.

The shrimp alkaline phosphatase enzyme was utilized to dephosphorylate any unused dNTPs from the primary PCR before the second allele-specific primary extension PCR. In the second PCR, 2μL of the reconstituted extension primer cocktail was added to each reaction well, and the following conditions were set: initial denaturation at 94°C for 30 sec, 40 cycles of one step at 94°C for 5 sec with 5 sub-cycles

of 52°C for 5 sec and 80°C for 5 sec, and a final extension at 72°C for 3 min. The extension products were conditioned using resin, and 10 nL was dispensed into a 384-well sample microtiter plate using the MassARRAY Nanodispenser RS1000 (Agena Bioscience). The module controls the MassARRAY Analyzer Compact to acquire spectra from SpectroCHIPs. As each SpectroCHIP is processed by the Compact, the spectral data is automatically processed, and saved to the MassARRAY database. The mass spectra were then acquired and analyzed with MassARRAY Typer 4.0 software. The average concordance rate for the 46 SNPs was higher than 98.7% based on 96 blind comparisons.

To mitigate the impact of potential confounding effects which might introduce bias, we employed the following methods: 1) Matching and restriction, which involve the stringent selection of patients with sPE and normal pregnant women. This ensures that the two groups are similar in terms of factors like age and weight, thereby minimizing the influence of other potential factors. 2) We employed multivariate logistic regression analysis to analyze the structured data and derive the corresponding *P*-values. This helps reduce model complexity and effectively accounts for the influence of various confounding factors. 3) We select values with a minor allele frequency (MAF) between 0.01 and 0.05, and *P*-values less than 0.05, as the optional range. MAF values that are too small result in poor reliability, while values that are too large often have no survival selection differences. 4) We remove sites with poor quality and those that are not in the exon region. Even for exon chip, there are still many sites outside of the exon region. 5) We search for sites with odds ratios (*OR*) >1 and *P*<0.05, or *OR*<1 and *P*<0.05. Find literature corresponding to each gene and assess the relationship between the gene and PE.²⁹

Mouse biometric measurements

Blood pressure was measured using the intelligent and non-invasive Blood Pressure Meter BP-2010 (Softron Biotechnology, Beijing, China). Gestation timing was established by mating the mice and checking for vaginal plugs. The morning on which a plug was observed was marked as E0.5. The females were preconditioned by measuring their baseline blood pressure at the same time every day (2 p.m.) before they were mated with males. The blood pressure of the mated mice was then measured at 2 p.m. on E8.5, E10.5, E12.5, E14.5, and E18.5. During the measurement process, the mice were immobilized in a holder on a heating platform to maintain their tail skin temperature at 38°C throughout the measurement process, according to the following parameters: five preconditioning data and 10 regular data. The blood pressure value was determined by taking the average of the five preconditioning data and 10 regular data, after removal of any outliers.⁶⁴ All measurements for each mouse, from preconditioning to routine cycles after pregnancy, were conducted in the same channel with the same cuffs to minimize inter-channel and cuff variation. Mouse Albumin ELISA Kit (Sigma-Aldrich, Saint Louis, Missouri, USA) and Creatinine (urinary) Colorimetric Assay Kit (Cayman Chemical, Ann Arbor, Michigan, USA) were used according to the manufacturer's instructions. Concentrations were determined by measuring the absorbances of the samples and standards at a wavelength of 450 nm with a microplate reader (Molecular Devices, Silicon Valley, California, USA). The albumin-to-creatinine ratio was then calculated.

Transmission electron microscopy (TEM)

For TEM analysis, we isolated 1mm³ kidney samples, which were then fixed in 2.5% glutaraldehyde at room temperature for 2-3 h and stored at 4°C. Subsequently, the samples were rinsed five times for 15 min each time using a sodium dihydrogen phosphate and disodium hydrogen phosphate buffer (0.1M, pH=7.4), followed by fixation in 1% osmium tetroxide for 1.5 h in the dark. The samples were then dehydrated using ethanol and acetone, penetrated with resin, and embedded with resin. Ultrathin tissue sections (65nm) were then prepared and stained with 2% uranyl acetate and lead citrate for 25 min and 7 min, respectively. Finally, the sections were washed, baked under infrared light for 10 min, and observed using a transmission electron microscope (Hitachi Limited, Tokyo, Japan). Each group consisted of at least three mice.

Artificially induced decidualization

The vasectomized males were prepared by removing 0.5 cm of their vasa deferentia while they were under anesthesia induced by 4% chloral hydrate. The males' sterility was confirmed by mating them with fertile females and observing the absence of pregnancy in the females with copulatory plugs. To prepare pseudopregnant females, the vasectomized males were then mated with the females in a 1:2 ratio. At E4, the pseudopregnant females were anesthetized with chloral hydrate and one uterine horn was injected with 25μL of sesame oil (Sigma-Aldrich) to induce decidualization, while the other remained untreated to serve as a control. The mice were sacrificed at E7.5, and the weight of the oil-injected uterine horns was compared to the untreated controls, and ratios were calculated for each mouse. The tissues were collected from the uterine horns and either fixed in 4% paraformaldehyde (Servicebio Biotechnology Co., Ltd., Wuhan, Hubei, China) or snap-frozen in liquid nitrogen for storage until further analysis.⁶⁵

RNA sequencing (RNA-Seq) and data analysis

Total RNA was extracted from the samples using the Trizol reagent (Invitrogen, Carlsbad, California, USA), followed by rRNA removal. The RNA libraries were constructed using the TruSeq Stranded Total RNA Library Prep Kit (Illumina), following the manufacturer's instructions. To ensure optimal quality, the libraries were quality-controlled with Agilent 2200 and sequenced using NovaSeq 6000 (Illumina) with a 150 bp paired-end run. To obtain clean reads, adapter sequences and low-quality reads were eliminated from the raw reads before read mapping. The clean reads were then aligned to the mouse genome (NCBI) with the Hisat2.⁶⁶ Fold change and *P*-values were calculated based on RPKM, and differentially expressed mRNA was identified. *P*-value and *FDR* analysis were subjected to the following criteria: i), fold change>2 or <0.5; ii), *P*<0.05, *FDR*<0.05. Gene ontology (GO) analysis was performed based on the differentially expressed mRNAs.⁶⁷ GO annotations were

downloaded from NCBI (<http://www.ncbi.nlm.nih.gov/>), UniProt (<http://www.uniprot.org/>), and Gene Ontology (<http://www.geneontology.org/>). Fisher's exact test was applied to identify the significant GO categories ($P < 0.05$).

Histological analysis and immunohistochemistry

The placenta, kidney, and artificially induced decidua of mice were dissected and fixed in 4% paraformaldehyde at 4°C overnight. The fixed tissues were then embedded in paraffin and sectioned at a thickness of 7 μm. Subsequently, the sections were dewaxed with xylene and rehydrated using an alcohol gradient (100%, 95%, 85%, 75%, 65%, 55%) before being stained with hematoxylin and eosin (H&E) (Solarbio Science & Technology Co., Ltd., Beijing, China) for 10 sec each. Finally, the samples were dehydrated with an alcohol gradient and transparentized twice with xylene before being mounted with neutral gum (Sinopharm Chemical Reagent Co., Ltd, Shanghai, China). Morphological observation and polyploid analysis of decidual cells were conducted using an automatic digital slide scanner (3D HISTECH, Budapest, Hungary).

For immunohistochemistry, the tissue sections were first dewaxed and rehydrated using xylol and a graded alcohol series containing decreasing concentrations of ethanol. The antigen retrieval process was then initiated by heat treatment in citrate buffer. To prevent interference from endogenous peroxidase activity, the sections were treated with 3% H₂O₂ for 15 min, followed by blocking with primary antibody diluent (Servicebio Biotechnology) for 1 h. The sections were then incubated with rabbit anti-IL-11R α antibody (1:200, HuaBio Biotechnology Co., Ltd, Hangzhou, Zhejiang, China) overnight at 4°C. After washing the sections three times with PBS, the sections were incubated with goat anti-rabbit secondary antibody (1:200, ZSGB-BIO Biotechnology Co., Ltd. Beijing, China) for 1 h at room temperature. Next, the sections were washed three times with PBS and developed using a DAB kit (ZSGB-BIO) to generate positive signals. Hematoxylin was used for counterstaining, and the subsequent steps of dehydration, transparentization, and mounting were performed as outlined earlier in this section. Images were captured using an automatic digital slide scanner (3D HISTECH), and the quantification of the staining results was expressed as the average optical density (AOD), analyzed through ImageJ 1.4.3.67 software (Media Cybernetics, Silver Spring, MD, USA).

Quantitative polymerase chain reaction (qPCR) analysis

Total RNA was extracted using TRIzol reagent (Invitrogen) and reverse transcribed with a cDNA synthesis kit (Yeastar Biotechnology Co., Ltd, Shanghai, China) following the manufacturer's instructions. The resulting cDNAs were then amplified through qPCR with the addition of SYBR Green Master Mix (Yeastar) in a Light Cycler Real-Time PCR instrument (Roche, Basel, Switzerland) following the specifications provided by the manufacturer. QPCR was conducted under the following conditions: a 5 min period at 95°C, followed by 35 cycles of 30 sec at 95°C, 30 sec at 58°C, 30 sec at 72°C, and a 10 min extension at 72°C. Gene expression changes were normalized to *Actb* and analyzed by the 2^{- $\Delta\Delta C_t$} method. The primer sequences can be found in [Table S1](#).

Western blot

The total proteins extracted from the tissue were obtained using RIPA buffer (Beyotime Biotechnology Co., Ltd., Shanghai, China), which contained PMSF (Beyotime Biotechnology Co., Ltd.) to inhibit protease degradation. Next, the samples were separated via electrophoresis on an SDS-PAGE gel (Solarbio Biotechnology) and then transferred onto polyvinylidene fluoride membranes (Millipore, Boston, Massachusetts, USA). Afterward, the membranes were incubated with one of the primary antibodies (IL-11R α , 1:500 dilution, HuaBio Biotechnology Co., Ltd.; GP130, 1:500 dilution, ABclonal, Wuhan, China; NSUN5, 1:500 dilution, Thermo Fisher, Waltham, Massachusetts, USA; JAK2, 1:1000 dilution, ABclonal; P-JAK2, 1:500 dilution, ABclonal; STAT3, 1:1000 dilution, ABclonal; P-STAT3, 1:500 dilution, ABclonal; CD3, 1:1000 dilution, HuaBio Biotechnology Co., Ltd.; and β -actin, 1:5000 dilution, HuaBio Biotechnology Co., Ltd.) overnight at 4°C. Next, a horseradish peroxidase-labeled secondary antibody (Thermo Fisher) was added and incubated for 1 h at room temperature. Lastly, the protein bands were developed using a chemiluminescence detection kit (Millipore, Bedford, MA, USA), and the relative intensities of the bands were determined using Quantiscan software (Biosoft, Cambridge, United Kingdom).

RNA immunoprecipitation (RIP) assay

The RIP procedure was carried out using the RNA Immunoprecipitation Kit (Geneseed, Guangzhou, Guangdong, China) in accordance with the manufacturer's instructions. Briefly, the collected tissue samples were lysed in RIP lysis buffer, followed by centrifugation at 14000g for 10 min at 4°C. The supernatant was then incubated in RIP buffer containing magnetic beads that had been cross-linked with antibodies targeting NSUN5 (Thermo Fisher) or control IgG (HuaBio Biotechnology Co., Ltd.) at 4°C for 5 h. The beads were then washed and the complexes were incubated with RIP buffer and purified through a column. The protein and RNA obtained were analyzed by Western blot and qPCR as described above.

QUANTIFICATION AND STATISTICAL ANALYSIS

All data were analyzed using the GraphPad Prism software (GraphPad Software, San Diego, California, USA). The results are presented as mean \pm SEM values. The differences between the groups were assessed with a Student's *t*-test and a *P*-value of less than 0.05 was considered statistically significant.